IJE TRANSACTIONS B: Applications Vol. 39, No. 02, (February 2026) 511-522

International Journal of Engineering

Journal Homepage: www.ije.ir

Segmentation of Brain Tumors from Magnetic Resonance Imaging with k-means Clustering Morphological Local and Global Intensity Fitting

M. Kazemi, H. Farsi*, S. Mohamadzadeh, A. Barati

Department of Electrical and Computer Engineering, University of Birjand, Birjand, Iran

PAPER INFO

Paper history:
Received 10 February 2025
Received in revised form 23 February 2025
Accepted 15 June 2025

Keywords:
Brain Tumor
Segmentation
Morphological
Active Contour
Magnetic Resonance Imaging

ABSTRACT

The precise detection of brain tumors in magnetic resonance imaging (MRI) is crucial for diagnosis and therapy planning. Conversely, conventional approaches often face challenges such as intensity changes, complex tumor shapes, and susceptibility to noise. This study introduces a novel hybrid framework that integrates histogram matching, k-means clustering, and a Morphological Local and Global Intensity Fitting (MLGIF) model to tackle these issues. The first stage in histogram matching is normalizing the intensity distributions of MRI data. K-means clustering is used to provide an initial segmentation of the tumor regions. The MLGIF-based active contour model enhances the precision of tumor border segmentation while maintaining computational economy by integrating both local and global intensity inputs. The BraTS 2013 dataset was used to conduct comprehensive evaluations to determine the efficacy of the suggested framework. The Dice coefficient was 94.18%, while the Jaccard index was 89.11%. The results demonstrated that our method effectively segmented brain tumors and had promise for real-world therapeutic applications.

doi: *10.5829/ije.2026.39.02b.17*

Graphical Abstract

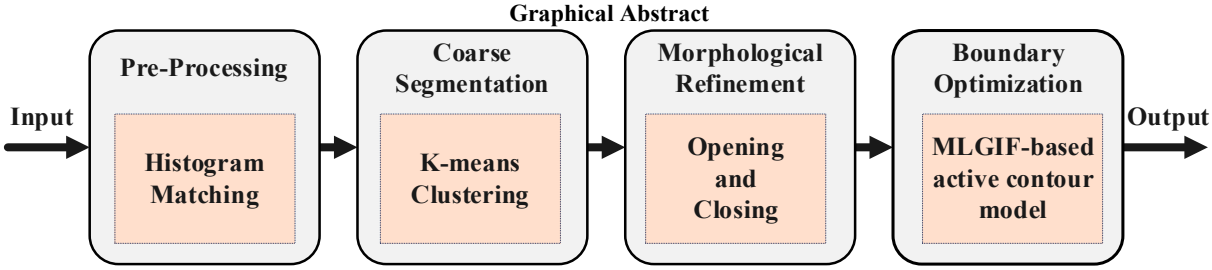

1. INTRODUCTION

Medical image processing is fundamentally reliant on the segmentation of brain tumors from MRI images, which affects diagnosis, treatment planning, and patient prognosis. Accurate tumor delineation is essential for identifying tumor margins, estimating volume, and tracking disease progression, hence assisting healthcare practitioners in making educated choices. Achieving enhanced segmentation accuracy remains a considerable challenge due to the complex attributes of tumor morphology (in terms of shape and size) and the presence of anomalies such as noise and inhomogeneities in MRI data. MRI is regarded as the superior imaging technique for assessing brain tumors, offering improved contrast resolution and accurate visualization of soft tissues, while eliminating exposure to ionizing radiation for patients. Multimodal MRI sequences, including T1-weighted, T2-weighted, T1 with contrast enhancement (T1c), and Fluid-Attenuated Inversion Recovery (FLAIR), provide complementary insights into various tumor characteristics, facilitating a comprehensive assessment. Although manual segmentation is the standard procedure in clinical environments, it is time-consuming, labor-intensive, and susceptible to variability among various observers as well as the same observer at different times.

*Corresponding Author Email: hfarsi@birjand.ac.ir (H. Farsi)

Please cite this article as: Kazemi M, Farsi H, Mohamadzadeh S, Barati A. Segmentation of Brain Tumors from Magnetic Resonance Imaging with k-means Clustering Morphological Local and Global Intensity Fitting. International Journal of Engineering, Transactions B: Applications. 2026;39(02):511-22.

Consequently, the need for automated brain tumor segmentation methods with computing economy and accuracy is become more obvious.

Many techniques have been developed to address the challenges of brain tumor segmentation over history. Edge detection methods, region-growing strategies, k-means and fuzzy c-means, although traditional approaches, have shown promise frequently encounter issues linked with irregular tumor morphologies.

Conversely, machine learning methodologies, particularly those using convolutional neural networks (CNNs) such as U-Net, have attained remarkable outcomes in recent years (1-3). These models are proficient at recognizing complicated patterns from extensive labeled datasets and are especially adept at segmenting tumors with sophisticated features. Nonetheless, deep learning methodologies need substantial training on meticulously annotated datasets, which are often scarce in medical imaging. Furthermore, they may be computationally demanding and susceptible to variations in imaging procedures and scanner configurations. To address these issues, hybrid segmentation algorithms that integrate traditional image processing methods with sophisticated computer models have garnered heightened interest. These approaches aim to use the benefits of both methodology; classic techniques provide efficient and robust initial segmentation, but modern methods such as active contour models (ACMs) update tumor borders to improve accuracy.

This study presents a novel hybrid framework for brain tumor segmentation using FLAIR-weighted MRI images, derived from the BraTS 2013 dataset. The method begins with preprocessing in which histogram matching is used for intensity normalizing. By ensuring that intensity distributions across pictures match a standard reference, histogram matching reduces variances brought about by scanner settings and imaging techniques. This improves stability in contrast levels, therefore enabling more consistent segmentation findings across multi-institutional datasets. This stage reduces discrepancies arising from changes in scanner settings or imaging techniques, thereby enhancing the robustness of the segmentation process. Subsequently, k-means clustering is used to provide an approximate localization of the tumor region. The estimated tumor border functions as the preliminary contour for a Morphological Active Contour Model (ACM) augmented by the Morphological Local and Global Intensity Fitting (MLGIF) technique. The MLGIF method enhances tumor identification by using both local and global intensity data, particularly in images exhibiting intensity homogeneity. In contrast to traditional ACMs primarily reliant on global intensity attributes (such as the Chan-Vese model), the MLGIF model employs localized morphological features to improve tumor delineation. Our dual-level intensity fitting maintains high accuracy, reduces computational costs, and ensures precise segmentation over varying contrast levels. Employing morphological approximations substantially decreases the computational expense of the final ACM equations while preserving excellent boundary delineation accuracy.

The suggested method attains Dice and Jaccard coefficients of 94.18% and 89.11%, respectively, illustrating its efficacy in precise and computationally economical brain tumor segmentation. The remainder of the paper is organized as follows: Section 2 reviews related works. Section 3 details the proposed methodology. Section 4 presents experimental results. Section 5 concludes the study with potential future directions.

2. RELATED WORK

Computer-aided tumor identification and segmentation systems provide effective options for reducing the diagnostic load on doctors. In recent years, several automated brain tumor segmentation approaches have evolved, exhibiting varied performance results across clinical studies (4-7). Contemporary methodologies are often categorized into three paradigms: 1) supervised learning models, 2) unsupervised clustering algorithms, and 3) hybrid structures that amalgamate both approaches (8-10).

Supervised segmentation methods depend on annotated datasets or established anatomical knowledge to adjust to novel situations (11-14). Despite the time-consuming nature of manual annotation, these methods have shown significant efficacy in identifying tumor areas. They can be broadly classified into generative and discriminative models (15-18). Generative methods use intensity distributions from MRI images with anatomical priors inside statistical frameworks, recognizing cancers as statistical anomalies by contrasting them with healthy tissue profiles based on morphology or signal patterns (19, 20). In contrast, discriminative methods rely on supervised classifiers such as support vector machines (21, 22), and random forests (23), leveraging multimodal MRI-derived features spanning intensity values, geometric properties, and spatial asymmetry.

Deep learning methodologies, especially convolutional neural networks (CNNs), have shown exceptional efficacy in tumor segmentation (24). Architectures such as U-Net and DeepMedic use encoder-decoder frameworks and skip connections to capture complex tumor characteristics. Research has shown that Dice similarity coefficients of 90% have been achieved by CNN-based approaches in tumor segmentation tasks. Nonetheless, these techniques need comprehensive annotated datasets, demand significant

computing resources, and exhibit sensitivity to discrepancies in imaging procedures and scanner settings, hence limiting their generalizability. CNNs often encounter difficulties with tiny or diffuse tumor areas, necessitating data augmentation and domain adaption strategies to improve their resilience.

Unsupervised methods function autonomously from labeled training data. Clustering techniques (e.g., k-means, FCM) classify pixels into cohesive areas based on feature similarity metrics (e.g., pixel intensity, texture patterns) (25). Simultaneously, energy-minimization techniques such as active contours segment structures via the iterative optimization of energy functions. Since its inception by Kass et al. (26), active contour models have evolved into parametric and geometric variations (e.g., level sets), becoming indispensable in 3D medical image analysis owing to their adaptability in managing topological alterations (27, 28). Nonetheless, these techniques encounter difficulties with intensity fluctuations, noise, and intricate tumor shapes, hence limiting their efficacy in demanding segmentation tasks. Conventional active contour models sometimes need human initialization, rendering them less suitable for completely automated applications.

Hybrid approaches combining deep learning with traditional methods have emerged as a potential fix for both of their drawbacks. Fooladi et al. (29) for instance integrated CNNs with Fuzzy K-Means clustering using deep feature extraction in line with cluster-based area segmentation. Their approach beat clustering and solo CNN with a Dice coefficient of 91.5%. Emadi et al. (30) suggested a technique that integrates super-pixel segmentation with the Fast Primal Dual Algorithm to improve the accuracy of brain tumor diagnosis in MRI data. Their methodology shown substantial improvements in managing noise and intensity fluctuations. Nouri and Damavandi (31), suggested a significant hybrid method that employs a texture segmentation technique employing a parametric active contour model driven by energy reduction grounded in Jensen-Tsallis Divergence. This method obtained exact segmentation of complex regions by effectively combining active contour models with texture analysis.

While Shahvaran et al. (28) used k-means clustering with Gaussian distribution modeling, surpassing existing contour-based methods on the BraTS 2013 dataset with a reported Dice score improvement of 3–5%, Shekari and Rostamian (32) more recently used FCM clustering with morphological reconstruction and active contour models to improve robustness against noise. These hybrid approaches show how well classical and deep learning methods could be used to enhance segmentation performance.

Transformer-based models, attention processes, and semi-supervised learning underlie recent developments in brain tumor segmentation: Often surpassing CNN-based approaches in situations needing contextual knowledge, transformer systems such as Swin-UNET and TransBTS capture long-range dependencies and have demonstrated encouraging outcomes in medical imaging. By dynamically weighting important information and hence enhancing border delineation, attention-based networks like Attention U-Net improve segmentation accuracy. Using both labeled and unlabeled data, semi-supervised learning methods provide a viable path to help with data shortage issues. Consistent regularity and self-training have been used successfully to reduce dependence on completely annotated datasets while maintaining competitive segmentation accuracy.

Notwithstanding these developments, some difficulties still exist including reliance on large labeled datasets, computational inefficiencies, and the necessity of models resistant to changes in imaging techniques. With an eye toward enhanced accuracy and computational efficiency in brain tumor segmentation, this work addresses these gaps by proposing a hybrid framework combining histogram matching, k-means clustering, and an LGIF-based active contour model. Our method aims to provide competitive Dice and Jaccard coefficients while lowering computing cost by using the strengths of clustering for first segmentation and LGIF-based active contour refining.

With a Dice coefficient of 94.18% and a Jaccard index of 89.11%, the recommended method shows strong performance and is thus very relevant in clinical environments. This study has significant therapeutic consequences as it improves tumor segmentation accuracy and efficiency. Therefore, helping radiologists and doctors to plan treatments and diagnose diseases.

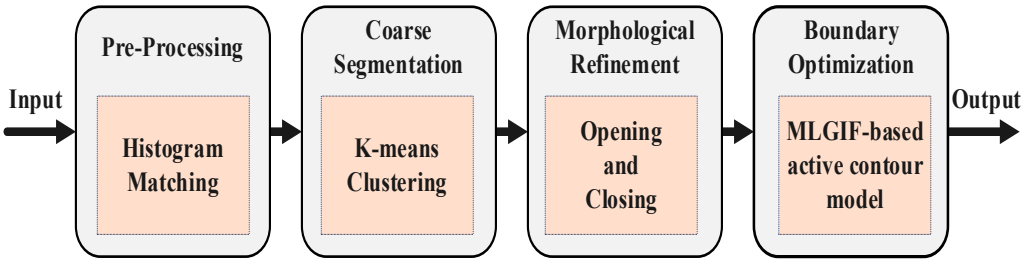

Figure 1. Proposed method for Segmentation of brain tumors

3. PROPOSED ALGORITHM

Segmentation of brain tumors in MRI is a challenging endeavor affected by variables like intensity inhomogeneity, uneven tumor shape, and susceptibility to noise. This paper presents a hybrid segmentation system that amalgamates many strategies to improve robustness and accuracy, addressing these challenges. Our approach achieves accurate boundary delineation by means of histogram matching for intensity normalization, K-means clustering for initial segmentation, morphological reconstruction for structural enhancement, and an advanced active contour model predicated on morphological local and global intensity fitting.

Designed as a sequential pipeline including four main stages: pre-processing, clustering, morphological refinement, and boundary optimization. Figure 1 shows the suggested approach. Furthermore, Algorithm 1 uses MR images to define the pseudo-code for the tumor identification process, therefore describing the necessary computational phases in segmentation.

Algorithm 1: Proposed Brain Tumor Segmentation

Input: Flair-weighted MRI volume
Output: Segmented tumor mask
1. **Pre-processing:**
   - Normalize intensities via histogram matching.
2. **Coarse Segmentation:**
   - Cluster image into **K=2** regions using K-means (Eq.1).
3. **Morphological Refinement:**
   - Remove false positives via opening operation (Eq.3).
   - Fill tumor cavities via closing operation (Eq.4).
4. **Boundary Optimization:**
   - Initialize active contour using refined mask.
   - Evolve contour via MLGIF energy minimization (Eq.9).
5. **return** Final tumor mask.

3. 1. Pre-processing In image processing, histogram matching is a method used to modify the intensity distribution of an input picture so that it aligns with a reference image with intended contrast characteristics. This method guarantees that the input picture takes on the visual traits of the reference image, hence improving consistency across datasets.

Medical imaging carefully selects the reference picture to show great contrast between tumor areas and healthy tissues, particularly for tumor identification. Matching the histogram of the input picture to this reference helps tumor regions to be more distinct, hence enabling effective segmentation and analysis. Standardizing MRI images from different scanners or protocols depends on this step, which makes sure that activities that happen later on in the computer system work the same way every time.

3. 2. Clustering To efficiently localize tumor regions in Flair-weighted MRI scans, we partition the pre-processed image into two clusters using K-means clustering. This simplified clustering strategy is motivated by the inherent hyperintensity of tumors in Flair-weighted MRI, which naturally distinguishes tumor tissue from surrounding brain parenchyma. The objective function minimizes intra-cluster variance:

$$J = \sum_{i=1}^{2} \sum_{x \in C_i} \|x - \mu_i\|^2 \quad (1)$$

where μ_i represents the centroid of cluster C_i. The tumor candidate is the cluster with the greater mean intensity. Although this binary partitioning offers a crude segmentation, it is computationally effective prior to downstream refinement using the MLGIF active contour model. Every centroid is updated repeatedly using:

$$c_j = \frac{1}{m_j} \sum_{i \in c_j} x_i, \quad 1 \le j \le \ell \quad (2)$$

where C_j is the centroid of cluster j, calculated as the average location of all data points x_i connected with that cluster, while m_j specifies the total count of data points inside cluster j. We indicate the number of clusters by j. Iteratively performed, the centroid update equation refines each cluster center and lets the algorithm converge toward an ideal clustering result. Using the MLGIF active contour model, this formulation provides a strong beginning for further segmentation refinement and is especially helpful in separating the picture into tumor and non-tumor areas.

3. 3. Morphological Refinement Essential methods in image processing that improve segmentation outcomes by changing pixel values depending on spatial relations are morphological operations. These procedures eliminate useless areas and assist in maintaining structural integrity. More complex processes like opening and closure are based on the main morphological changes, dilatation, and erosion.

Minimizing false positives and raising the accuracy of the found tumor areas depend on morphological opening and closure procedures within the framework of tumor segmentation. Small non-tumor features, including edema and vascular components, are removed using an opening procedure including an erosion stage followed by dilation. This is shown mathematically as follows:

$$I_{Opening}: \quad I \circ S = (I \Theta S) \oplus S \quad (3)$$

where S denotes a structuring element with a disk-like shape. After this stage, a morphological closure is done to restore the overall shape of the tumor and seal minor gaps resulting from the opening surgery. This procedure entails dilation followed by erosion applied on the previously refined tumor mask:

$$I_{Closing}: \ I_{Opening} \bullet S = (I_{Opening} \oplus S) \Theta S \quad (4)$$

By means of repetitive application of these processes, a more coherent tumor mask is obtained, therefore augmenting the starting basis for the active contour model in the next segmentation step. By eliminating unnecessary areas and smoothing borders, morphological reconstruction improves the tumor mask and guarantees more uniformity for the active contour initiation. Two crucial pictures are used in this operation: the mask image, which shows the first segmentation, and the marker image, acquired by means of morphological changes aimed at eliminating unwelcome features. The ensuing improved tumor mask is then used to provide a strong basis for the active contour model.

3. 4. Boundary Optimization Active contour models (ACMs) have found extensive use in medical picture segmentation due to their ability to actively and adaptively develop outlines. Inspired by geometric flows and surface evolution theory, these models minimize an energy functional generated from picture characteristics, hence refining object bounds. Using intensity homogeneity, one of the most well-known region-based active contour models, the Chan-Vese model (33), effectively segments objects. Common problems in medical imaging, however, this model finds difficult with weak borders and intensity inhomogeneity.

Fouladivanda et al. (27) suggested the LGIF model, a complex active contour framework that combines local morphological information with global intensity consistency into a coherent energy functional, to go over these limitations. This method enhances the global region-based Chan-Vese model by extending upon the Local Morphology Fitting (LMF) framework developed by Sun et al. (34), hence enhancing segmentation efficiency in pictures showing significant intensity variations. Moreover, the MLGIF model guarantees computational efficiency by using the optimization strategy suggested by Márquez-Neila et al. (35), hence retaining robustness against noise and artifacts.

The fundamental premise of MLGIF is the integration of both local and global energy components, enabling the model to adjust to diverse intensity distributions within the image. The energy functional of MLGIF is articulated as follows:

$$E_{MLGIF} = \alpha E_{CV} + (1-\alpha) E_{LMF} \quad (5)$$

The weighting parameter $\alpha \in [0,1]$ dynamically modifies the impact of local and global terms inside the energy functional. It is characterized as follows:

$$\alpha(x) = \tau.\text{average}\,(CR_W(x)).(1 - CR_W(x)) \quad (6)$$

In this context, τ represents a positive constant, whereas $CR_W(x)$ denotes the local contrast index computed within a neighborhood window W centered at the pixel x. The local contrast index $CR_W(x)$ is defined by:

$$CR_W(x) = \frac{I_W^{\max} - I_W^{\min}}{I_r} \quad (7)$$

$I_W^{\max}$ and $I_W^{\min}$ represent the maximum and minimum intensity values within the neighborhood window W, whereas I_r serves as a scaling factor for normalizing the contrast index. The Chan-Vese energy functional, functioning as the global term in MLGIF, is defined as follows:

$$\begin{aligned} E_{CV} &= \mu.(\text{lenght}(\varphi)) + \nu.(\text{area}(\varphi)) \\ &+ \lambda_1 \int_{inside(C)} \|I(x) - c_1\| dx \\ &+ \lambda_2 \int_{outside(C)} \|I(x) - c_2\| dx \end{aligned} \quad (8)$$

where C represents the evolving contour, whereas c_1 and c_2 reflect the average intensities within and outside the contour, respectively. The weighting coefficients λ_1 and λ_2 regulate the influence of intensity variations. The parameters length (C) and area inside (C) set limitations on the contour's smoothness and dimensions. The Chan-Vese model proficiently represents global intensity distributions but fails to accommodate local fluctuations, which are essential in medical imaging impacted by intensity inhomogeneity.

Fouladivanda et al. (27) proposed a local energy term derived from morphological operations to boost segmentation in scenarios of non-uniform intensity, hence improving flexibility to spatial intensity fluctuations. The comprehensive energy functional of MLGIF is articulated as follows:

$$\begin{aligned} E_{MLGIF} &= \mu.(\text{lenght}(\varphi)) + \nu.(\text{area}(\varphi)) \\ &+ \alpha\{\lambda_1 \int_{inside(C)} \|I(x) - c_1\| dx \\ &+ \lambda_2 \int_{outside(C)} \|I(x) - c_2\| dx\} \\ &+ (1-\alpha)\{\lambda_3 \int_{inside(C)} \|I(x) - f_1(x)\| dx \\ &+ \lambda_4 \int_{outside(C)} \|I(x) - f_2(x)\| dx\} \end{aligned} \quad (9)$$

where $f_1(x)$ and $f_2(x)$ denote fuzzy membership functions that illustrate local intensity distributions, while λ_3 and λ_4 regulate the impact of the local energy components. By integrating these local morphological characteristics into the segmentation process, MLGIF significantly improves contour evolution, guaranteeing accurate border recognition even in pictures with substantial intensity fluctuations.

The segmentation procedure utilizing MLGIF adheres to a systematic methodology. An initial tumor mask is created and utilized as input for the active contour model. The contour evolution is executed by

reducing the MLGIF energy functional, hence progressively refining the tumor boundaries. During each iteration, morphological operations, including opening and closure, are employed to preserve structural integrity. The initial operation eliminates minor, extraneous structures, whereas the concluding procedure fills voids and maintains the connectedness of the tumor area. This repeated approach persists until convergence is achieved, guaranteeing that the final contour precisely corresponds with the tumor boundaries.

The MLGIF model offers substantial benefits compared to conventional segmentation techniques. Integrating both global and local intensity data promotes resilience to intensity inhomogeneity and diminishes false positives. Moreover, the integration of morphological operators enhances computational efficiency and guarantees contour stability. These attributes render MLGIF exceptionally appropriate for medical imaging applications, notably in MRI-based tumor segmentation, where intensity fluctuations and indistinct borders frequently present significant hurdles.

4. EXPERIMENTAL RESULTS

This section presents the experimental findings of our suggested hybrid framework for brain tumor segmentation. The experiments were performed on the BraTS 2013 dataset to assess the accuracy and efficacy of our technique. The results are structured systematically to align with the study objectives and facilitate clear interpretation.

4. 1. Materials The BraTS 2013 dataset serves as a prominent baseline for brain tumor segmentation. From people diagnosed with gliomas, the dataset consists of multimodal MRI scans (T1, T2, T1c, and FLAIR), including low-grade and high-grade cases. The dataset displays a range of tumor attributes regarding shape, size, and intensity variations. Every image is accompanied by manually annotated ground truth labels supplied by experienced radiologists, utilized for assessing the efficacy of segmentation algorithms. Additionally, the dataset is partitioned into training and testing subsets to guarantee an equitable comparison of various segmentation techniques.

4. 2. Evaluation Metrics This research employs the following measures to assess the efficacy of our proposed method: Dice Similarity Coefficient (DSC), Intersection over Union (IoU), Precision (Pr), and Sensitivity (S). DSC assesses the congruence between the predicted segmentation and the ground truth, whereas IoU evaluates the resemblance between the predicted and real tumor areas. Precision denotes the ratio of accurately predicted tumor pixels to the total predicted tumor pixels, whereas Sensitivity (Recall) quantifies the ratio of accurately predicted tumor pixels to the total real tumor pixels.

The mathematical expressions of these metrics are as follows:

$$DSC=\frac{2\times|X\cap Y|}{|X|+|Y|} \tag{10}$$

$$IoU=\frac{|X\cap Y|}{|X\cup Y|} \tag{11}$$

$$Pr=\frac{TP}{TP+FP} \tag{12}$$

$$Se=\frac{TP}{TP+FN} \tag{13}$$

Whereas Y denotes the gathering of ground truth tumor pixels (reference segmentation), X denotes the segmentation outcome that is, the predicted tumor pixels. True Positives (TP) are indicated by $|X\cap Y|$, the count of pixels where the ground truth and expected segmentations line-up. While $|Y|$ represents the total count of ground truth tumor pixels, which includes TP and False Negatives (FN), $|X|$ symbolizes the total count of expected tumor pixels, which includes True Positives (TP) and False Positives (FP). TP denotes pixels precisely identified as tumor; TN, or True Negatives, are pixels properly categorized as non-tumor; FP denotes pixels mistakenly projected as tumor; FN denotes pixels from the ground truth tumor zone not detected as tumor in the prediction.

4. 3. Configuration The suggested approach was assessed using the BraTS 2013 dataset. Our tests concentrated on FLAIR-weighted MRI sequences because of their enhanced contrast for identifying edema and defining tumor margins, especially in the Whole Tumor (WT) area. The FLAIR sequence is particularly adept in delineating hyperintense regions linked to tumors and edema, rendering it an appropriate option for segmenting the whole tumor region. The findings indicate that our approach attains competitive performance in precisely outlining tumor locations, validating the effectiveness of concentrating on FLAIR-weighted pictures for brain tumor segmentation.

The experiments were conducted using a 5-fold cross-validation strategy to ensure the robustness and generalizability of the results. The parameters for the MLGIF model were optimized through extensive experimentation and set as follows: $W = 7$, $\tau = 4$, $\mu = 1$, $\lambda_1 = 5\times10^{-4}$, $\lambda_2 = 3\times10^{-4}$, λ_3,$\lambda_4 = 10^{-4}$ and $\nu = 0$. These parameters were carefully selected to balance the trade-off between segmentation accuracy and computational efficiency.

TABLE 1. Dice, Jaccard, Precision and Sensitivity metrics

Image ID (Slice Number)	MLGIF				Proposed method (HM+K-Means+MLGIF)			
	DSC	IoU	Pr	Se	DSC	IoU	Pr	Se
BraTS2013_0_1 (75)	64.48	47.57	100	47.57	90.03	81.86	86.31	94.07
BraTS2013_1_1 (56)	47.14	30.84	30.84	100	91.94	85.09	97.11	87.30
BraTS2013_2_1 (112)	75.97	61.26	61.65	98.97	91.68	84.64	87.69	96.05
BraTS2013_3_1 (86)	84.71	73.48	76.78	94.48	91.10	83.66	91.28	90.93
BraTS2013_4_1 (66)	79.14	65.48	71.04	89.31	91.80	84.85	91.03	92.59
BraTS2013_5_1 (91)	86.99	76.97	93.20	81.55	95.73	91.81	96.69	94.79
BraTS2013_6_1 (100)	93.48	87.76	99.74	87.97	97.02	94.22	98.72	95.38
BraTS2013_7_1 (102)	95.06	90.59	99.44	91.05	97.59	95.30	98.29	96.90
BraTS2013_8_1 (81)	79.29	65.68	66.11	99.03	93.95	88.59	95.52	92.43
BraTS2013_9_1 (100)	80.61	67.52	98.21	68.36	94.07	88.80	92.95	95.21
BraTS2013_10_1 (85)	80.59	67.49	77.75	83.65	92.05	85.28	96.11	88.33
BraTS2013_11_1 (104)	93.54	87.86	88.61	99.04	96.07	92.44	93.99	98.25
BraTS2013_12_1 (86)	71.03	55.08	99.85	55.12	97.71	95.53	97.68	97.74
BraTS2013_13_1 (80)	85.02	73.95	73.95	100	95.71	91.77	94.04	97.44
BraTS2013_14_1 (85)	92.90	86.74	98.24	88.11	95.64	91.65	95.75	95.54
BraTS2013_15_1 (100)	23.81	13.52	13.58	96.60	87.35	77.54	78.48	98.48
BraTS2013_16_1 (93)	89.52	81.03	85.19	94.32	93.50	87.80	93.54	93.47
BraTS2013_17_1 (112)	90.94	83.39	84.58	98.33	94.89	90.27	96.28	93.54
BraTS2013_18_1 (105)	88.94	80.09	93.78	84.58	95.04	90.55	98.73	91.62
BraTS2013_19_1 (115)	67.27	50.68	92.65	52.81	93.14	87.16	98.31	88.49
BraTS2013_20_1 (115)	88.57	79.48	95.15	82.84	94.92	90.33	96.80	93.11
BraTS2013_21_1 (90)	93.14	87.16	98.31	88.49	96.07	92.43	97.94	94.26
BraTS2013_22_1 (86)	82.81	70.67	79.43	86.50	96.72	93.65	97.13	96.32
BraTS2013_23_1 (109)	92.78	86.53	96.28	89.52	95.95	92.22	98.30	93.71
BraTS2013_24_1 (95)	78.40	64.48	86.54	71.66	94.39	89.37	90.05	99.17
BraTS2013_25_1 (108)	89.86	81.59	85.48	94.71	95.91	92.14	98.38	93.57
BraTS2013_26_1 (105)	90.31	82.32	82.72	99.42	95.44	91.28	96.29	94.61
BraTS2013_27_1 (75)	87.08	77.11	92.50	82.26	93.64	88.05	94.16	93.14
BraTS2013_28_1 (76)	87.52	77.80	99.00	78.42	89.13	80.39	97.72	81.93
BraTS2013_29_1 (101)	94.07	88.80	99.87	88.91	97.16	94.47	96.51	97.81
Means	**81.83**	**71.43**	**84.02**	**85.79**	**94.18**	**89.11**	**94.73**	**93.87**

4. 4. Quantitative Results Several performance measures including the Dice Similarity Coefficient (DSC), Jaccard Index (IoU), Precision, and Sensitivity were used to evaluate the suggested approach. These measures were chosen to assess the segmentation technique's accuracy holistically. Table 1 shows the advantages attained by including histogram matching, k-means clustering, and the MLGIF-based active contour model by a comparison of the proposed technique to the MLGIF methodology.

With a mean Jaccard index of 89.11% and a mean Dice coefficient of 94.18%, the suggested approach far exceeded the MLGIF technique. Furthermore noted were the mean Precision and Sensitivity levels, at 93.87% and 94.73% respectively. These gains suggest that the suggested structure guarantees better segmentation accuracy while efficiently lowering false positives and false negatives, thereby preserving computational economy.

Table 1 especially shows that, throughout all tested slices, the suggested approach always exceeded the MLGIF model. For one of the BraTS dataset slices, for example, the Dice coefficient for the suggested strategy was 95.04%, whereas the DHCP method had 88.94%. This contrast emphasizes how well the suggested approach precisely defines tumor borders, particularly in situations with notable intensity uniformity or irregular tumor shapes.

The capacity of the suggested approach to more efficiently manage fluctuations in tumor shape and intensity distributions than LGIF is a main benefit. The increases in Precision and Sensitivity ratings point to the method's very skillful ability to lower misclassifications, a critical consideration in medical imaging applications where lowering false positives and false negatives directly influences clinical decision-making.

The findings in Table 1 demonstrate, with great accuracy and robustness, that the suggested segmentation approach has great possibilities for practical use in clinical settings. The approach is a good fit for inclusion into automated medical diagnostic systems as it can efficiently segment brain tumors while preserving a balance between accuracy and computing economy. Moreover, the consistency of findings over many slices suggests that the method is generalizable and may be used on many datasets without appreciable performance reduction.

These results show that the suggested framework addresses important issues such intensity fluctuations, tumor boundary abnormalities, and segmentation stability, therefore offering significant advantages over standard segmentation methods. While the increased Precision and Sensitivity ratings show the method's practical relevance in clinical and research environments, the strong Dice and Jaccard coefficients demonstrate its dependability.

4. 5. Comparison with Other Methods To further validate the effectiveness of the proposed method, we evaluated its performance against other advanced segmentation techniques, as shown in Table 2. With a mean Dice coefficient of 94.18%, the suggested approach exceeded other published approaches like nnU-Net (88.95%), 2DResU-Net with ResBlock (90%), and U-Net coupled with Adaptively Regularized Kernel-Based Fuzzy C-Means and Level Set (93%).

Particularly in situations with complicated tumor forms, the increases in Dice and Jaccard scores show that our method offers greater segmentation accuracy. Unlike earlier techniques that suffer from intensity changes, our approach uses histogram matching, which greatly improves the resilience of segmentation across many MRI images.

4. 6. Qualitative Results Figure 2 presents the segmentation results for a given input picture, therefore highlighting the qualitative findings of the proposed approach. The image highlights how exactly tumor boundary lines are constructed in multiple sample slices. In these graphic outputs, yellow pixels represent True Positives (TP), red pixels show False Positives (FP), and green pixels show False Negatives (FN).

TABLE 2. Compared proposed method with other methods

Ref	Method	Dateset	DSC
(36)	GANs + diffusion models	BraTS2020	90
(37)	Autoencoder + Attention Gates	BraTS2021	90.82
(38)	nnU-Net	BraTS2020	88.95
(39)	2DResU-Net + ResBlock	BraTS2018	90
(40)	Inception U-Det	BraTS2017	86.8
(41)	U-Net + FCM + Level set	BraTS2017	93
(42)	RF+ ACM	BraTS2013	89
(28)	Morphological ACM	BraTS2013	91.79
(32)	FCM + ACM	BraTS2013	93.07
Our method	**HM + K-means + MLGIF**	**BraTS2013**	**94.18**

The suggested method has a major benefit in terms of increased accuracy in recording tumor margins, hence reducing both FP and FN mistakes. As seen in the second and third columns of Figure 2, our approach significantly lowers incorrect classifications when compared to MLGIF. Red and green pixel counts suggest that the suggested method effectively and more precisely detects the tumor area.

Furthermore clear evidence of our approach's strength is its capacity to manage complicated tumor forms and intensity changes. Unlike LGIF, which usually causes mistakes in areas with varying intensity levels, our approach efficiently addresses such difficulties and preserves segmentation quality. This quality is especially important for brain tumor segmentation, in which tumors show variable intensity distributions and irregular forms.

Moreover, our approach enhances small tumor preservation as the fourth and fifth rows of Figure 2 reveal. LGIF finds it difficult to exactly capture these small structures; sometimes leading to either incomplete omission (false negatives) or over-segmentation (false positives). The proposed method clearly characterizes such regions even while maintaining a balanced segmentation output.

These results illustrate how effectively our approach generates correct, constant, robust tumor segmentation, hence it is a superior alternative for MLGIF under demanding medical imaging situations.

Moreover, Figure 3 shows in MRI images the progressive processing and assessment of the suggested tumor segmentation strategy. While the second row (b)

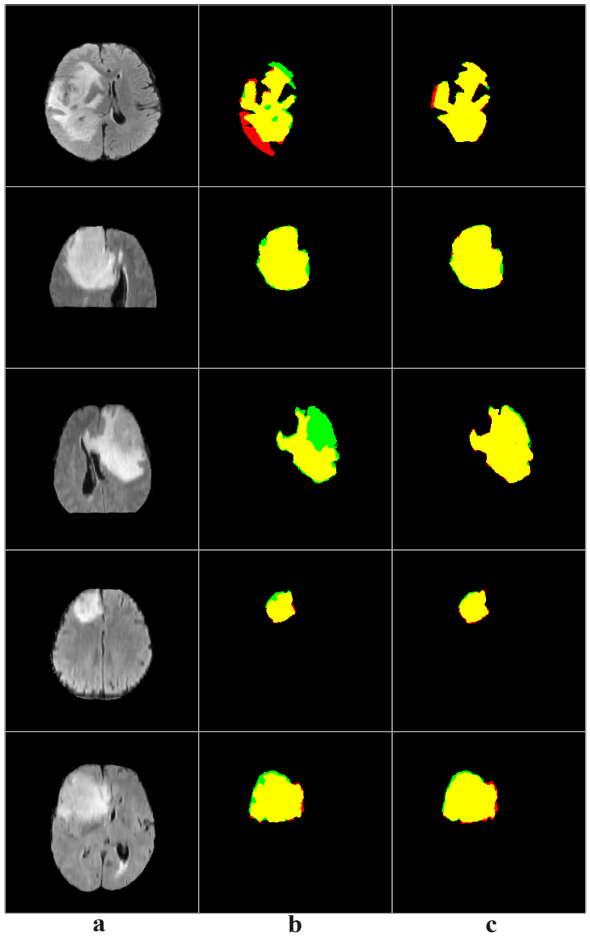

Figure 2. Segmentation outcomes: (a) input, (b) MLGIF, and (c) our approach. Yellow denotes true positives (TP), red signifies false positives (FP), and green indicates false negatives (FN)

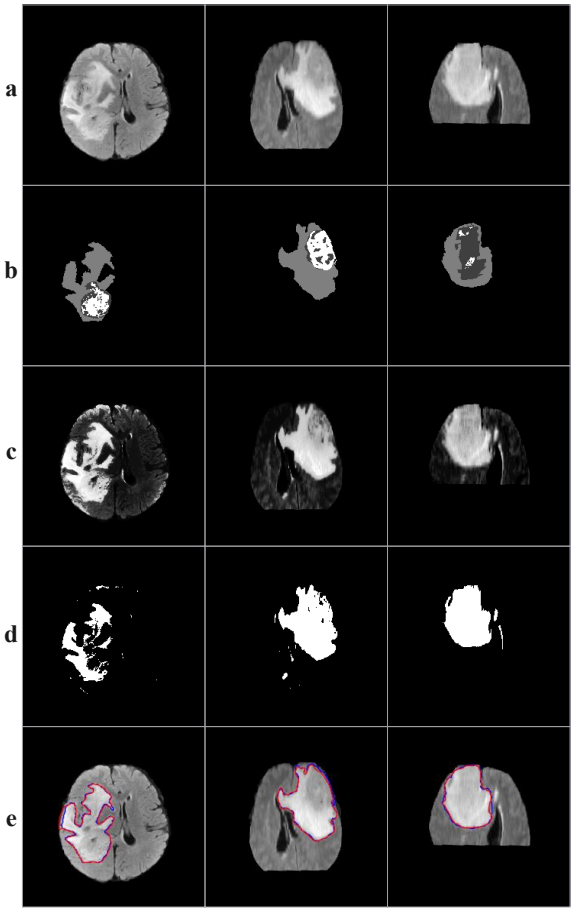

Figure 3. Outcomes of the suggested methodology: (a) Input, (b) Ground Truth, (c) Histogram matching output, (d) K-means Clustering result, (e) Comparative analysis of the suggested approach against Ground Truth (red: MLGIF outcome, blue: Ground Truth)

shows the manually segmented Ground Truth, acting as the standard for assessing the segmentation accuracy, the first row (a) shows the raw MRI inputs. Histogram matching is used in row (c) to improve the contrast and intensity consistency thereby increasing the pictures' similarity to the training data. Though it captures tumor areas, the fourth row (d) displaying the segmentation outcome achieved using the K-means clustering technique indicates noise and partial segmentation problems.

At conclusion, row (e) provides a direct comparison between the proposed method (MLGIF) where red contours indicate the MLGIF output and the Ground Truth segmentation shown by blue contours. The results reveal that the proposed method works better than K-means clustering and closely matches the expert-annotated Ground Truth in exactly delineating tumor boundaries. The comparison highlights how precisely the proposed technique performs segmentation, therefore supporting its use for MRI image tumor detection.

4. 7. Discussion The experimental findings indicate that the suggested strategy attains superior performance in brain tumor segmentation. The integration of histogram matching, k-means clustering, and the MLGIF-based active contour model enables the technique to proficiently address intensity inhomogeneity, uneven tumor margins, and noise. Figure 4 presents a detailed, stepwise visualization of the suggested methodology, illustrating the output at each phase comprehensively. The elevated Dice and Jaccard scores, in conjunction with the high Precision and Sensitivity, indicate that the suggested technique is both precise and resilient.

A primary benefit of the suggested strategy is its computational efficiency. Utilizing morphological procedures and the MLGIF model, the approach decreases computer complexity while maintaining excellent segmentation accuracy. A detailed analysis of this complexity reduction is provided by Fouladivanda et al. (27). This makes it appropriate for real-time clinical

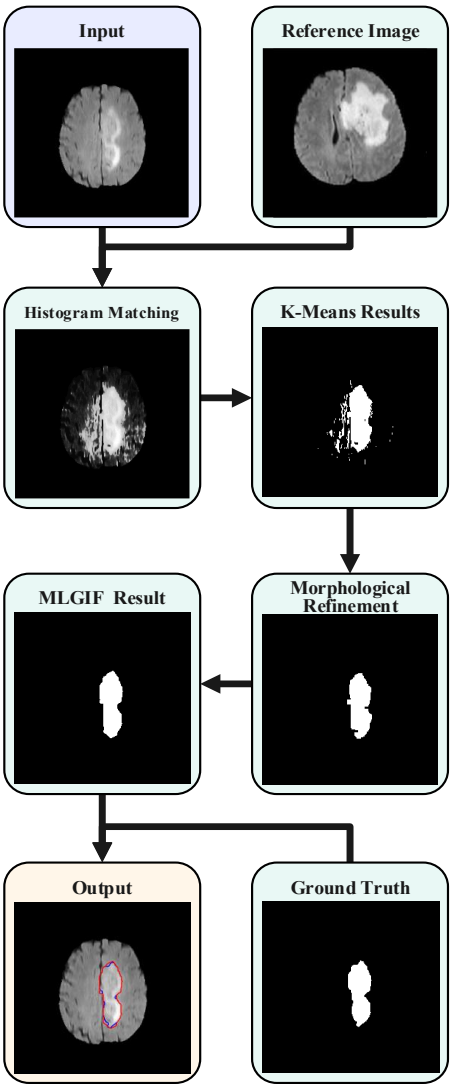

Figure 4. A processed brain MRI from the BraTS2013 dataset, with segmentation and delineated tumor region

applications, where both precision and rapidity are essential.

Nonetheless, the suggested technique has several drawbacks. For example, its efficacy may fluctuate when used on datasets exhibiting substantial disparities in imaging procedures or tumor attributes. Subsequent research may concentrate on improving the method's generalizability by the integration of adaptive approaches and the examination of bigger, more heterogeneous datasets.

5. CONCLUSION

This research introduces an innovative hybrid framework for brain tumor segmentation in MRI images, using histogram matching for intensity normalization, k-means clustering for initial tumor localization, and an active contour model based on MLGIF for accurate border refining. The suggested technique efficiently tackles issues associated with intensity fluctuations, noise, and intricate tumor shapes. Experimental assessments on the BraTS 2013 dataset indicate that the suggested methodology attains a mean Dice coefficient of 94.18% and a Jaccard index of 89.11%, exceeding other established techniques. The enhanced Precision and Sensitivity demonstrate the method's efficacy in properly delineating tumor locations while reducing false positives and false negatives.

The suggested approach is computationally effective, which qualifies for real-time therapeutic uses. Moreover, its resistance to noise and intensity inhomogeneities improves its possible incorporation into clinical procedures, thereby giving doctors consistent segmentation results to support diagnosis and treatment planning.

Though it performs rather well, several difficulties still exist. Future research should concentrate on improving generalizability by means of training on bigger, more varied datasets and adaptive learning approaches. Furthermore enhancing segmentation accuracy and lowering dependency on large-scale labeled datasets might be achieved by using transformer-based designs and semi-supervised learning techniques.

Finally, our work emphasizes how well merging conventional and deep learning methods performs for brain tumor segmentation. A viable option for practical medical uses, the suggested hybrid technique not only enhances segmentation accuracy but also provides computing economy.

Data availability: The dataset used in this investigation is accessible via the BraTS 2013 repository at https://www.smir.ch/BRATS/Start2013

6. REFERENCES

1. Farsi H, Ghermezi D, Barati A, Mohamadzadeh S. Improving Deep Learning-based Saliency Detection Using Channel Attention Module. International Journal of Engineering Transactions B: Applications. 2024;37(11):2367-79. https://doi.org/10.5829/IJE.2024.37.11B.21
2. Mohamadzadeh S, Pasban S, Zeraatkar-Moghadam J, Shafiei AK. Parkinson's disease detection by using feature selection and sparse representation. Journal of Medical and Biological Engineering. 2021;41(4):412-21. https://doi.org/10.1007/s40846-021-00626-y
3. Sahragard E, Farsi H, Mohamadzadeh S. Advancing semantic segmentation: Enhanced UNet algorithm with attention mechanism and deformable convolution. PloS one. 2025;20(1):e0305561. https://doi.org/10.1371/journal.pone.0305561
4. Ahishakiye E, Bastiaan Van Gijzen M, Tumwiine J, Wario R, Obungoloch J. A survey on deep learning in medical image

reconstruction. Intelligent Medicine. 2021;1(03):118-27. https://doi.org/10.1016/j.imed.2021.03.003

5. Wadhwa A, Bhardwaj A, Verma VS. A review on brain tumor segmentation of MRI images. Magnetic resonance imaging. 2019;61:247-59. https://doi.org/10.1016/j.mri.2019.05.043
6. Mohammed YM, El Garouani S, Jellouli I. A survey of methods for brain tumor segmentation-based MRI images. Journal of Computational Design and Engineering. 2023;10(1):266-93. https://doi.org/10.1093/jcde/qwac141
7. Bauer S, Wiest R, Nolte L-P, Reyes M. A survey of MRI-based medical image analysis for brain tumor studies. Physics in Medicine & Biology. 2013;58(13):R97. https://doi.org/10.1088/0031-9155/58/13/R97
8. Dorrani Z, Farsi H, Mohamadzadeh S. Shadow Removal in Vehicle Detection Using ResUNet-a. Iranica Journal of Energy & Environment. 2023;14(1):87-95. https://doi.org/10.5829/ijee.2023.14.01.11
9. Rohani M, Farsi H, Mohamadzadeh S. Facial feature recognition with multi-task learning and attention-based enhancements. Iranica Journal of Energy & Environment. 2025;16(1):136-44. https://doi.org/10.5829/ijee.2025.16.01.14
10. Sezavar A, Farsi H, Mohamadzadeh S. A New Model for Person Reidentification Using Deep CNN and Autoencoders. Iranica Journal of Energy & Environment. 2023;14(4):314-20. https://doi.org/10.5829/ijee.2023.14.04.01
11. Daraei A, Hamidi H. An efficient predictive model for myocardial infarction using cost-sensitive J48 model. Iranian journal of public health. 2017;46(5):682.
12. Hamidi H, Vafaei A, Monadjemi SAH. Analysis and evaluation of a new algorithm based fault tolerance for computing systems. International Journal of Grid and High Performance Computing (IJGHPC). 2012;4(1):37-51. https://doi.org/10.4018/jghpc.2012010103
13. Hamidi H, Vafaei A, Monadjemi A. Algorithm based fault tolerant and check pointing for high performance computing systems. Journal of applied sciences. 2009;9(22):3947-56. https://doi.org/10.3923/jas.2009.3947.3956
14. Nilchi AN, Vafaei A, Hamidi H, editors. Evaluation of security and fault tolerance in mobile agents. 2008 5th IFIP International Conference on Wireless and Optical Communications Networks (WOCN'08); 2008: IEEE.
15. Mohammadi A, Hamidi H. Analysis and evaluation of privacy protection behavior and information disclosure concerns in online social networks. International Journal of Engineering, Transactions B: Applications. 2018;31(8):1234-9. https://doi.org/10.5829/ije.2018.31.08b.11
16. Asadi SAF, Hamidi H. An architecture for security and protection of big data. International Journal of Engineering, Transactions A: Basics. 2017;30(10):1479–86. https://doi.org/10.5829/ije.2017.30.10a.08
17. Hamidi H, Vafaei A, Monadjemi A. A framework for fault tolerance techniques in the analysis and evaluation of computing systems. International journal of innovative computing, information and control. 2012;8(7):5083-94.
18. Hamidi H. A model for impact of organizational project benefits management and its impact on end user. Journal of Organizational and End User Computing (JOEUC). 2017;29(1):51-65. https://doi.org/10.4018/JOEUC.2017010104
19. Bakas S, Reyes M, Jakab A, Bauer S, Rempfler M, Crimi A, et al. Identifying the best machine learning algorithms for brain tumor segmentation, progression assessment, and overall survival prediction in the BRATS challenge. arXiv preprint arXiv:181102629. 2018. http://arxiv.org/abs/1811.02629
20. Menze BH, Jakab A, Bauer S, Kalpathy-Cramer J, Farahani K, Kirby J, et al. The multimodal brain tumor image segmentation benchmark (BRATS). IEEE transactions on medical imaging. 2014;34(10):1993-2024. https://doi.org/10.1109/TMI.2014.2377694
21. Bauer S, Nolte L-P, Reyes M, editors. Fully automatic segmentation of brain tumor images using support vector machine classification in combination with hierarchical conditional random field regularization. International conference on medical image computing and computer-assisted intervention; 2011: Springer.
22. Kumar TS, Rashmi K, Ramadoss S, Sandhya L, Sangeetha T, editors. Brain tumor detection using SVM classifier. 2017 Third International Conference on Sensing, Signal Processing and Security (ICSSS); 2017: IEEE.
23. Breiman L. Random forests. Machine learning. 2001;45:5-32. https://link.springer.com/article/10.1023/A:1010933404324
24. Soomro TA, Zheng L, Afifi AJ, Ali A, Soomro S, Yin M, et al. Image segmentation for MR brain tumor detection using machine learning: a review. IEEE Reviews in Biomedical Engineering. 2022;16:70-90. https://doi.org/10.1109/RBME.2022.3185292
25. Sauwen N, Acou M, Van Cauter S, Sima D, Veraart J, Maes F, et al. Comparison of unsupervised classification methods for brain tumor segmentation using multi-parametric MRI. NeuroImage: Clinical. 2016;12:753-64. https://doi.org/10.1016/j.nicl.2016.09.021
26. Kass M, Witkin A, Terzopoulos D. Snakes: Active contour models. International journal of computer vision. 1988;1(4):321-31. https://doi.org/10.1007/BF00133570
27. Fouladivanda M, Kazemi K, Helfroush MS, Shakibafard A. Morphological active contour driven by local and global intensity fitting for spinal cord segmentation from MR images. Journal of neuroscience methods. 2018;308:116-28. https://doi.org/10.1016/j.jneumeth.2018.07.015
28. Shahvaran Z, Kazemi K, Fouladivanda M, Helfroush MS, Godefroy O, Aarabi A. Morphological active contour model for automatic brain tumor extraction from multimodal magnetic resonance images. Journal of neuroscience methods. 2021;362:109296. https://doi.org/10.1016/j.jneumeth.2021.109296
29. Fooladi S, Farsi H, Mohamadzadeh S. Segmenting the lesion area of brain tumor using convolutional neural networks and fuzzy k-means clustering. International Journal of Engineering, Transactions B: Applications. 2023;36(8):1556-68. https://doi.org/10.5829/IJE.2023.36.08B.15
30. Emadi M, Dehkordi ZJ, Mobarakeh MI. Improving the accuracy of brain tumor identification in magnetic resonanceaging using super-pixel and fast primal dual algorithm. International Journal of Engineering, Transactions A: Basics. 2023;36(3):505-12. https://doi.org/10.5829/ije.2023.36.03c.10
31. Nouri M, Damavandi YB. A New Texture Segmentation Method with Energy-driven Parametric Active Contour Model Based on Jensen-Tsallis Divergence. International Journal of Engineering, Transactions A: Basics. 2022;35(7):1257-67. https://doi.org/10.5829/ije.2022.35.07a.05
32. Shekari M, Rostamian M. Brain tumor segmentation from MRI using FCM clustering, morphological reconstruction, and active contour. Multimedia Tools and Applications. 2024;83(14):42973-98. https://doi.org/10.1007/s11042-023-17233-5
33. Chan TF, Vese LA. Active contours without edges. IEEE Transactions on image processing. 2001;10(2):266-77.
34. Sun K, Chen Z, Jiang S. Local morphology fitting active contour for automatic vascular segmentation. IEEE transactions on biomedical engineering. 2011;59(2):464-73. https://doi.org/10.1109/TBME.2011.2174362
35. Marquez-Neila P, Baumela L, Alvarez L. A morphological approach to curvature-based evolution of curves and surfaces.

IEEE Transactions on Pattern Analysis and Machine Intelligence. 2013;36(1):2-17. https://doi.org/10.1109/TPAMI.2013.106

36. Usman Akbar M, Larsson M, Blystad I, Eklund A. Brain tumor segmentation using synthetic MR images-A comparison of GANs and diffusion models. Scientific Data. 2024;11(1):259. https://doi.org/10.1038/s41597-024-03073-x
37. Schwehr Z, Achanta S. Brain tumor segmentation based on deep learning, attention mechanisms, and energy-based uncertainty predictions. Multimedia Tools and Applications. 2025:1-20. https://doi.org/10.1007/s11042-024-20443-0
38. Isensee F, Jäger PF, Full PM, Vollmuth P, Maier-Hein KH, editors. nnU-Net for brain tumor segmentation. Brainlesion: Glioma, Multiple Sclerosis, Stroke and Traumatic Brain Injuries: 6th International Workshop, BrainLes 2020, Held in Conjunction with MICCAI 2020, Lima, Peru, October 4, 2020, Revised Selected Papers, Part II 6; 2021: Springer.
39. Yang Y, Wang P, Yang Z, Zeng Y, Chen F, Wang Z, et al. Segmentation method of magnetic resonance imaging brain tumor images based on improved UNet network. Translational Cancer Research. 2024;13(3):1567. https://doi.org/10.21037/tcr-23-1858
40. Aboussaleh I, Riffi J, Mahraz AM, Tairi H. Inception-UDet: an improved U-Net architecture for brain tumor segmentation. Annals of Data Science. 2024;11(3):831-53. https://doi.org/10.1007/s40745-023-00480-6
41. Khosravanian A, Rahmanimanesh M, Keshavarzi P, Mozaffari S. Enhancing level set brain tumor segmentation using fuzzy shape prior information and deep learning. International Journal of Imaging Systems and Technology. 2023;33(1):323-39. https://doi.org/10.1002/ima.22792
42. Ma C, Luo G, Wang K. Concatenated and connected random forests with multiscale patch driven active contour model for automated brain tumor segmentation of MR images. IEEE transactions on medical imaging. 2018;37(8):1943-54. https://doi.org/10.1109/TMI.2018.2805821

Persian Abstract

چکیده

تشخیص دقیق تومورهای مغزی در تصویربرداری تشدید مغناطیسی (MRI) نقش اساسی در فرآیند تشخیص و برنامه‌ریزی درمان دارد. با این حال، روش‌های مرسوم با چالش‌هایی مانند تغییرات شدت تصویر، اشکال پیچیده تومورها و حساسیت به نویز مواجه هستند. این مطالعه یک چارچوب ترکیبی نوین را معرفی می‌کند که با ادغام تطبیق هیستوگرام، خوشه‌بندی k-means و مدل مورفولوژیکی برازش شدت محلی و جهانی (MLGIF)، این مشکلات را برطرف می‌سازد. در مرحله نخست، تطبیق هیستوگرام برای نرمال‌سازی توزیع شدت داده‌های MRI انجام می‌شود. سپس، الگوریتم خوشه‌بندی k-means به‌عنوان یک بخش‌بندی اولیه برای نواحی توموری به کار می‌رود. در ادامه، مدل کانتور فعال مبتنی بر MLGIF دقت بخش‌بندی مرزهای تومور را با حفظ کارایی محاسباتی افزایش می‌دهد، زیرا ورودی‌های شدت محلی و جهانی را هم‌زمان در نظر می‌گیرد. برای ارزیابی جامع کارایی چارچوب پیشنهادی، از مجموعه داده BraTS 2013 استفاده شده است. نتایج نشان می‌دهد که روش ارائه‌شده تومورهای مغزی را با دقت بالایی بخش‌بندی می‌کند و پتانسیل بالایی برای کاربردهای درمانی در دنیای واقعی دارد. ضریب دایس ۹٤.۱۸٪ و شاخص جاکارد ۸۹.۱۱٪ به‌دست آمده است.